IOP Publishing Superconductor Science and Technology
Supercond. Sci. Technol. **34** (2021) 045010 (7pp) https://doi.org/10.1088/1361-6668/abe4b5

High normal zone propagation velocity in copper-stabilized 2G HTS coated conductors

Jaël Giguère, Christian Lacroix, Félix Dupuis-Desloges, Jean-Hughes Fournier-Lupien and Frédéric Sirois

Polytechnique Montréal, Montréal, QC H3C 3A7, Canada

E-mail: christian.lacroix@polymtl.ca and f.sirois@polymtl.ca

Received 5 October 2020, revised 21 December 2020
Accepted for publication 9 February 2021
Published 25 February 2021

Abstract

Copper-stabilized second generation high-temperature superconductor (HTS) coated conductors were modified to enhance their normal zone propagation velocity (NZPV). Experimental results, supported by numerical simulations, indicate that adding copper on the substrate side instead of adding it on the HTS side increases the NZPV by a factor of 2–3. Furthermore, a novel tape architecture, called hybrid-current flow diverter (CFD), was investigated. This hybrid-CFD tape was designed with the goal of having a very long current transfer length, which is the key to enhance the NZPV. Results show that it is possible to fabricate an HTS tape with double stabilizer thickness in comparison to a bare tape, while accelerating the NZPV by a factor of three. With the same approach, a ten-fold increase of the NZPV can be expected for a tape with a 40 μm thick copper-stabilizer.

Keywords: quench, normal zone propagation velocity, 2G HTS coated conductors

1. Introduction

Second generation high-temperature superconductor coated conductors (2G HTS CCs), or simply high-temperature superconductor (HTS) tapes, are promising candidates for applications such as superconducting motors [1], compact wind generators [2], compact proton therapy systems [3] and compact fusion power plants [4]. However, present fabrication processes induce inhomogeneities in their properties along their length. As a results, the critical current can fluctuate locally by ≈20% around its average value. Therefore, when carrying a current close to the average critical current, a local quench can occur, which can lead to a degradation of the superconducting properties of the tape if no proper action is taken quickly enough.

In high field magnets, one way to reduce the risks of damaging HTS tapes upon a quench is to use the concept of non-insulated (NI) coils. This approach has proved to be very robust, even in high magnetic fields [5]. However, one important drawback with NI coils is their long charging time (from tens of seconds to minutes). In power applications though (e.g. superconducting motors), and in many other magnet applications, a long charging time is unacceptable, and one must revert to the more conventional insulated coil approach (i.e. each turn of the coil is electrically insulated from its neighbors). In this case, quench protection is very difficult. A thick stabilizer is required, but this reduces the normal zone propagation velocity (NZPV) of the tape, known to be very low in 2G HTS CCs [6–10]. An interesting avenue to improve quench protection is thus the enhancement of the NZPV using innovative concepts such as the use of a current flow diverter (CFD) in the tape [11, 12].

Up now, the CFD concept has been demonstrated experimentally on 2G HTS CCs with only 2 μm of silver for the stabilizer. However, for applications such as superconducting motors or generators, a thicker stabilizer is required to ensure proper tape robustness. In this paper, we demonstrate that the CFD concept can be used to enhance the NZPV in HTS tapes with a thick stabilizer. Two types of CFD architecture have been investigated: the bCFD architecture [13], where the buffer layers act as the CFD, and a hybrid-CFD architecture, which combines the bCFD approach and the 'traditional' CFD concept [11], implemented by inserting a patterned electrical resistance between the HTS and silver layers.

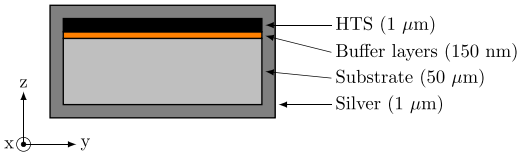

Figure 1. Architecture of a 2G HTS CC as manufactured by SuperPower Inc., also called 'bare tape' in this paper.

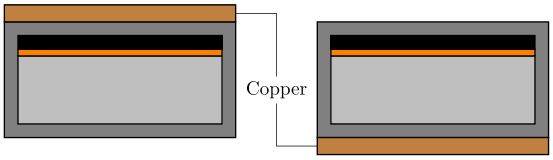

Figure 2. Left: tape architecture with copper on the HTS side (called 'TOP' architecture). Right: tape architecture with copper on the substrate side (called 'bCFD' architecture).

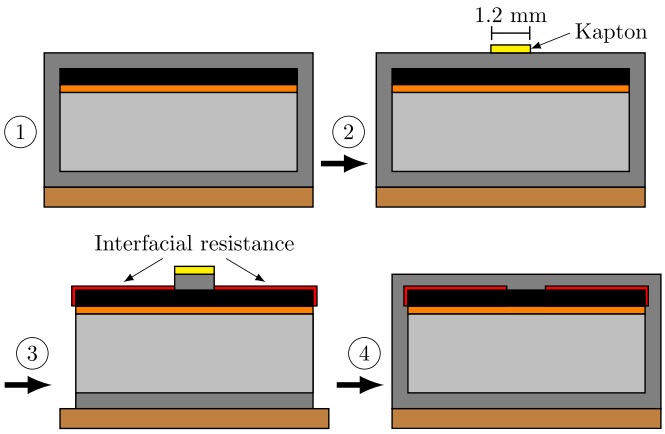

Figure 3. Fabrication steps of a hybrid-CFD tape. Step 1: addition of a copper stabilizer (3 μm thick) on the substrate side. Step 2: a kapton tape is used to mask a thin line of silver (1.2 mm wide) in the middle of the tape. Step 3: chemical etching of exposed silver, which creates a thin amorphous insulating layer at the surface of the HTS layer (thin red area). Step 4: sputtering of a 225 nm thick silver layer on the HTS layer and on the sides of the tape.

2. Sample fabrication

The experiments presented in this paper were realized on modified 4 mm wide commercial 2G HTS CCs fabricated by SuperPower Inc. [14]. The architecture of the base template is shown in figure 1. The tape consists of a 1 μm thick YBaCuO layer grown on a stack of buffer layers (150 nm thick) which were previously deposited on a Hastelloy substrate (50 μm thick). The whole tape is surrounded by a 1 μm thick silver layer. The critical current of the samples used in this work was between 132 and 141 A (77 K, self-field).

2.1. bCFD tapes

The bCFD tapes were fabricated by adding copper on the substrate side of the tapes. This was done by copper electroplating. A solution consisting of 20 ml l^{-1} of H_2SO_4 and 200 g l^{-1} $CuSO_4{\cdot}5H_2O$ and a current density of 30 mA cm^{-2} was used for electroplating. For each bCFD sample fabricated, another tape with the copper deposited on the HTS side (TOP) has been produced. In order to make sure the thickness of copper was exactly the same on both samples, the electrodeposition was realized simultaneously on the two samples. The architectures of both types of samples (bCFD and TOP) are shown in figure 2. A total of eight samples were fabricated (four bCFD samples and four TOP samples), with a copper thickness varying between 1 and 6 μm. Critical current measurements indicated that no degradation of the critical current occurred after the electroplating.

2.2. Hybrid-CFD tapes

Hybrid-CFD tapes, or simply hybrid tapes, consist in SuperPower bare tapes that have been modified to include a CFD at the HTS/Ag interface and a copper stabilizer on the substrate side. We called them hybrid tapes because their architecture includes a patterned resistance at the HTS/Ag interface (CFD) [15] and a thick stabilizer on the substrate side (bCFD) [13]. To create a hybrid tape, a 3 μm thick copper layer was first electroplated on the substrate side (see step 1 in figure 3). Secondly, an interfacial resistance between the HTS and Ag was created by realizing a chemical etching of the Ag layer, followed by an exposure of the HTS layer to ambiant air (steps 2 and 3 in figure 3). This is known to create a thin amorphous insulating layer (less than 6 nm thick) at the interface between HTS and Ag, as described in [15, 16]. A thin line of Ag in the middle of the tape (1.2 mm wide) was kept intact to ensure a good electrical contact (low interfacial resistance) between the HTS and the Ag at this location. In this work, the etching solution was composed of ammonium hydroxide and peroxide diluted in water in a volume ratio of 1:1:4, respectively. Finally, a 225 nm thick silver layer was sputtered on the HTS layer and on the sides of the tape to connect electrically the thin line of Ag remaining in the middle of the HTS layer with the electroplated copper layer on the substrate side (step 4 in figure 3, which also shows the final tape architecture). No degradation in the critical current of the tapes was observed after these modifications.

3. Measurement setup and experimental procedure

The NZPV of the tapes was measured using a homemade pulsed current source. Custom sample holders based on printed circuit boards (PCB) were fabricated in order to measure up to 38 differential voltages along 14 cm long HTS tapes. Because of PCB fabrication constraints, the voltage taps had to be arranged in a zigzag configuration (see figure 4). With this approach, the distance between the centers of two adjacent voltage taps can be as small as 1 mm. Each differential pair of voltage taps is called 'a*i*n', where $n = 2, 3, \ldots, 38$. A cylindrical NdFeB magnet was used to reduce locally the critical current of the sample to induce the initial quench (closed circle in figure 4).

To perform NZPV measurements, the sample was first immersed in a liquid nitrogen bath. Then, current pulses of

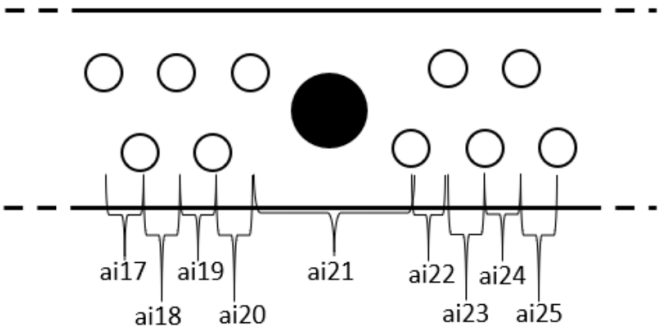

Figure 4. Schematic view of the arrangement of the voltage taps (open circles) used for NZPV measurements (top view). Each tap is separated horizontally and vertically by 1 mm from its neighbors. Each differential pair is labelled 'ai*n*', for 'analog input' *n*, where $n = 1, 2, \ldots, 38$. The closed circle in the middle represents the location of a magnetic defect created with a NdFeB magnet.

constant amplitude (close to each sample's I_c) and 5–30 ms long were applied in the sample. This current triggers a quench in the middle of the sample, where a small NdFeB magnet was placed to reduced the local critical current density. After the quench occurred, voltage drops start to appear between the voltage taps close to the quench, and with time, this voltage drop propagates toward both ends of the tape. The time evolution of all differential voltage measurements were recorded with a 80-channels data acquisition card from National Instruments. The NZPV was then calculated by taking the time delay between two adjacent ai*n* signals to reach a given voltage level, divided by the distance between the taps, here 1 mm. This measurement has been repeated for different current pulse amplitudes to obtain the dependance of the NZPV with the applied current. For more details about this procedure, see [11].

4. Experimental results

4.1. bCFD tapes

Figure 5 presents experimental results (symbols) and simulated values (full lines) of the NZPV versus applied current for selected samples (see legend for details). The simulations are discussed in the next section. The black squares correspond to NZPV measurements obtained on a bare SuperPower tape (see figure 1), used here as a comparison baseline. For the bare tape, the NZPV varies from 75 up to 175 cm s^{-1} for a current between 110 and 165 A. When a 2 μm thick copper layer is added on the substrate side (blue solar wheels, bCFD), the NZPV is reduced from 175 to 100 cm s^{-1} at 160 A. For comparison, when the 2 μm thick copper layer is added on the HTS side (red diamonds, TOP), the NZPV is reduced down to 50 cm s^{-1}, which is two times lower than the bCFD sample for the same amount of copper. A similar trend is obtained in the case of a 6 μm thick copper layer. For the bCFD tape, the NZPV is 70 cm s^{-1} for $I = 160$ A, while it is only 20 cm s^{-1} when the copper layer is put on the HTS side.

Figure 6 presents NZPV measurements (symbols) versus copper stabilizer thickness for an applied current of 160 A. We

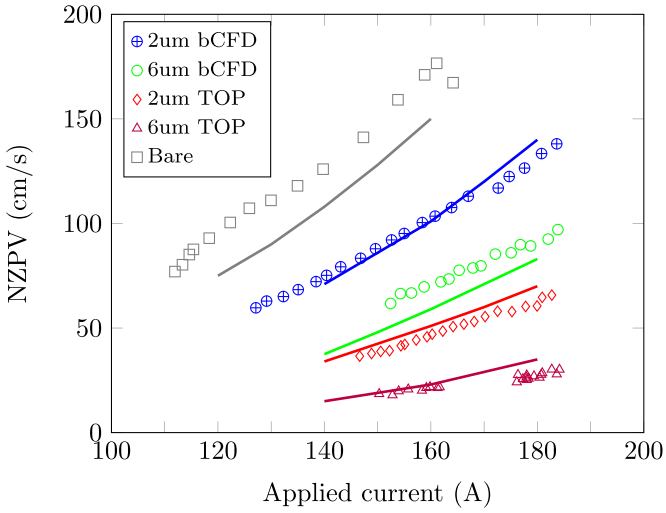

Figure 5. Measured (symbols) and simulated (full lines) values of NZPV as a function of current for different thicknesses of Cu stabilizer. Samples with copper layers of thicknesses of 2 and 6 μm (bCFD and TOP architectures) are compared to a bare commercial sample from SuperPower (black squares).

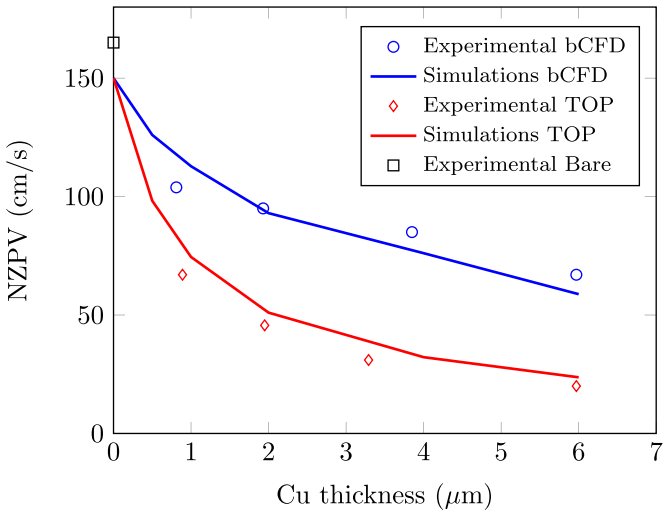

Figure 6. NZPV versus copper stabilizer thickness at a fixed current of 160 A. Symbols correspond to measurements, and full lines correspond to numerical simulation results.

observe that for both types of sample (bCFD and TOP), adding copper stabilizer reduces the NZPV, which is the expected behavior. However, the decrease is less drastic when the copper is placed on the substrate side (bCFD). Interestingly, a 6 μm thick copper layer located on the substrate side gives a NZPV similar to 1 μm thick copper layer located on the HTS side. These results demonstrate that the 'bCFD effect', observed previously on HTS tapes with a solely 2 μm thick silver stabilizer (see [13]), is also present when a thicker copper stabilizer is added on the substrate side.

4.2. Hybrid-CFD tape

The NZPV of a hybrid tape was measured for currents ranging from 80 to 170 A (red triangles in figure 7). We note that the

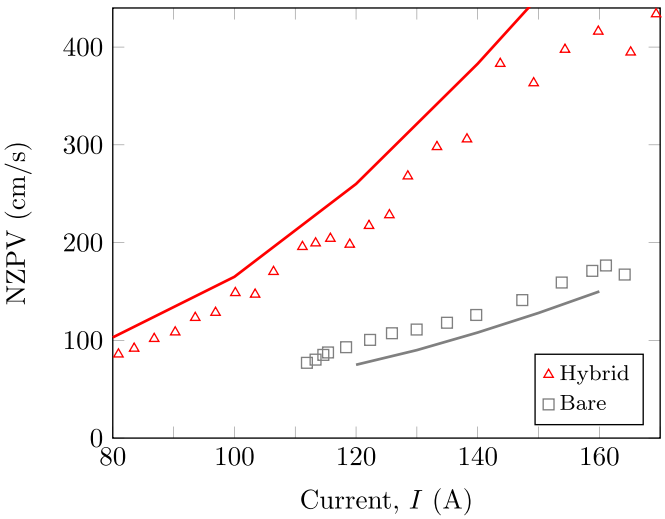

Figure 7. Measured (symbols) and simulated (full lines) values of NZPV as a function of current for a hybrid tape and for the SuperPower bare reference tape.

NZPV for $I = 160$ A is 400 cm s^{-1}, which is more than two times faster than for a bare tape at the same current amplitude. Furthermore, we recall that the hybrid tape has a 3 μm thick copper layer stabilizer, which is not the case for the bare tape.

5. Numerical simulations

All experiments have been reproduced by numerical simulations. The numerical simulations were performed with the Joule Heating module of the finite-element software COMSOL Multiphysics 4.3b. In short, the heat equation and the current continuity equation were solved simultaneously, coupled through the Joule losses and the temperature dependence of the material properties. The model used was the same as the one described in [12], except for the followings.

To emulate the reduction of the local critical current due to the magnetic field created by the cylindrical NdFeB magnet, a low J_c region was included in the simulated HTS tape. A gaussian shape was used to approximate the reduction in J_c induced by the magnet, instead of the heat pulse used in the model described in [12]. The critical current at $T = 77$ K used in the numerical simulations was 140 A, which corresponds to the average critical current measured in SuperPower tapes used in these experiments.

5.1. bCFD tapes

NZPV versus applied current curves for the bCFD tape architecture were obtained from the numerical simulations (solid lines in figures 5 and 6). A good agreement is observed between experiments and simulations. Since the bCFD effect has been investigated in details in [13], for the rest of the paper, we focus our analysis on the simulation results obtained for the hybrid tape architecture.

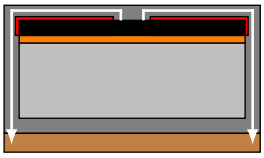

Figure 8. Upon a local quench, the current (white arrows) leaves the HTS layer by the middle of the tape, then flows in the top silver layer toward the edges, and it finally reaches the Hastelloy substrate, the bottom silver layer and the copper layer.

5.2. Hybrid-CFD tape

The hybrid tape was designed to maximize the current transfer length (CTL) when the current transfers from the HTS layer to the stabilizer or vice-versa upon the creation of a normal zone. Indeed, it was demonstrated earlier that the NZPV is proportional to the CTL [17]. As depicted in figure 8, upon a local quench, when the current leaves the HTS layer to go into the copper stabilizer, it must first come out of the HTS layer by the middle of the tape, then it must flow in the top silver layer to reach the edges of the tape, and it finally flows around the buffer layers and the substrate to reach the copper stabilizer. Note that a fraction of the current also goes into the substrate and the bottom silver layer.

In order to explain the quench mechanism occurring in the hybrid tape, numerical simulations were performed. First of all, to make sure that our numerical model was reliable, we compared the time evolution of the voltages obtained experimentally at a few specific pairs of voltage taps with those obtained from numerical simulations.

In figure 9(a), the measured voltages versus time is presented ($I = 106$ A). We observe that the voltage increases sharply in ai20, then it diminishes and starts to increase again. The same behavior is observed for adjacent pairs of voltage taps, with the difference that the peak amplitude of the voltage decreases as we move away from the magnetic defect. Note that in other tape architectures (commercial, CFD), when a quench occurs, the voltage increases monotonously with time. The overshoot of the voltage signal observed here is thus a new phenomenon, observed for the first time.

Next, we calculated the voltage versus time with our finite element model. We were able to reproduce very well the experimental behavior, as can be seen in figure 9(b). The reason why the peak value diminishes as we get far from the magnetic defect is because the voltage taps were not perfectly aligned with the tape during the experiment. In the numerical simulations, this misalignment had to be included to reproduce adequately the experiments. This gave us confidence in the model.

To help understanding the quench dynamics in hybrid-CFD tapes, the x-component of the electric field and the norm of current density in the middle of the tape along the x-direction were extracted for both the HTS layer and the top silver layer, see figure 10. We observe that the current density in the HTS layer increases sharply on the superconducting side of the superconducting phase/normal zone (SC/NZ) boundary. Similarly,

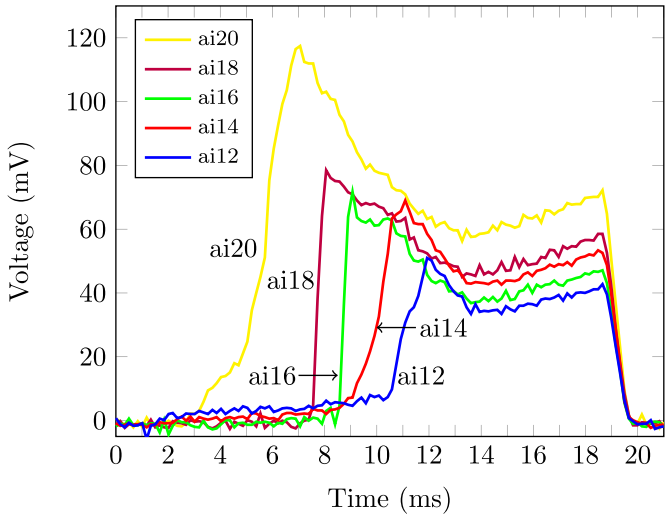

(a) Experimental

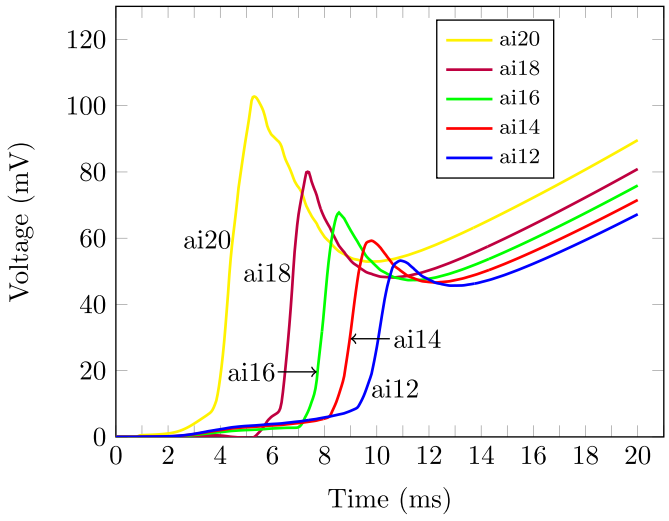

(b) Simulations

Figure 9. Voltage as a function of time for the hybrid tape ($I = 106$ A), showing the unexpected second rise in voltage after the first drop. Each 'ai' is a voltage measurement point on the tape.

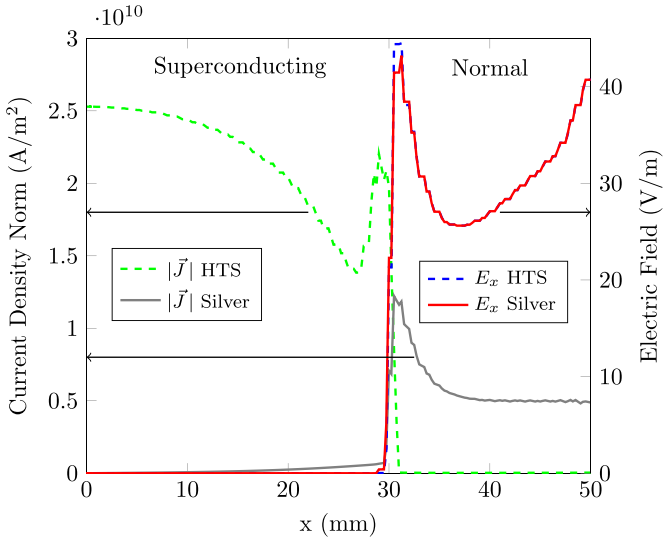

Figure 10. Norm of current density $\vec{J}$ and x-component of electric field $\vec{E}$ in the HTS layer and in the top silver layer, respectively, taken along the middle of the tape. The increase in electric field at $x = 31$ mm is due to current crowding, while the increase in electric field at $x = 50$ mm is due to a higher temperature induced by the low J_c region, at the defect location.

a peak is also observed in the current density in the top silver layer, this time, on the normal zone side of the SC/NZ boundary. Therefore, it is not surprising that the electric field E_x also shows a peak at this location, which explains the unusual time evolution of the voltage. Indeed, the peak in the voltage observed in figure 9 is due to a momentary increase in the current density (or momentary current crowding) in the middle of the tape, which translates in a momentary higher electric field and heat dissipation.

To further clarify the quench dynamics in hybrid tapes, 2D maps of the current density in the HTS layer and in the top silver layer are presented in figure 11. The arrows indicate the direction of the current, whereas the color map indicates the norm of the current density. A schematic of the hybrid tape is shown below each 2D map, with a blue solid line that indicates the position of the plane in which the plotted data were extracted.

We observe that, in the HTS layer, the current density reaches its maximum value in the middle part of the tape along the width, and exactly at the SC/NZ boundary. The current density is maximum at this location since the interfacial resistance between HTS and silver is the lowest, thus the current flows in the least resistance path, which causes a momentary current crowding. In other words, the current is forced to concentrate at this location in order to exit the HTS layer, before distributing itself in the other layers, as already shown in figure 8. The arrows in figure 11(a) clearly show this current crowding effect when it approaches the normal zone. Note that, as time evolves and normal zone expands, this current crowding moves to the left.

In the top silver layer (figure 11(b)), we observe that the current starts to flow in the silver much before reaching the normal zone, which corresponds to a large CTL. We note that in the center on the left, the current density is low but not zero ($\approx 10^9$ A m^{-2}). Furthermore, the direction of the arrows indicates that a significant fraction of the current is flowing perpendicular to the length of the tape (i.e. along the y direction) when it transfers from the HTS layer to the silver layer.

Figure 12 shows the fraction of the total current flowing in the x-direction in each layer of the tape near the SC/NZ boundary as a function of the position x along the length of the tape. We observe that the current falls to zero in the HTS layer at the SC/NZ boundary. Again, we observe that the current in the HTS starts to decrease long before reaching the normal zone. Similarly, the current starts to flow in the Hastelloy substrate, the bottom silver layer and the copper layer, long before reaching the SC/NZ boundary. In the normal zone,

(a) Current density in a x-y slice in the HTS layer.

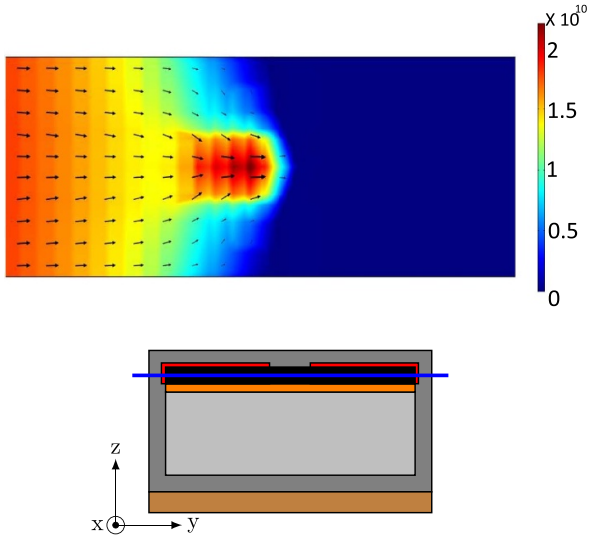

(b) Current density in a x-y slice in the top silver layer.

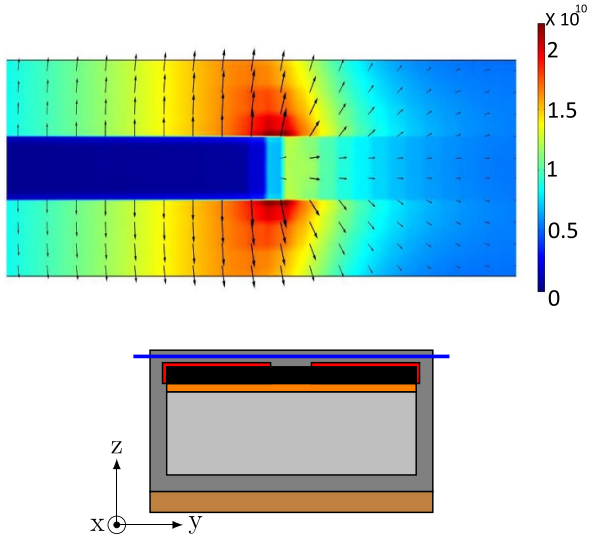

Figure 11. Two-dimensional maps of the current density (units: A m^{-2}) in selected layers of a hybrid tape during a quench. The width of the tape is 4 mm (y-direction) and the length shown is 18 mm along the x-direction. Below each two-dimensional map, a sketch of the tape architecture is shown where a blue line indicates the position of the x–y plane of the two-dimensional map. Current crowding is visible at the superconducting/normal zone boundary.

the biggest fraction of the current flows in the copper layer since it has the least resistance. We note that, in the case of the top silver layer, the current transfers at the SC/NZ boundary. In the literature, the CTL is defined as the length required for the current to change by a factor of e^{-1} from a specific boundary. Taking this boundary as the SC/NZ boundary, we obtain a CTL of 8 mm in our particular case, as indicated in figure 12. This CTL value is much larger than CTL in commercial tapes, which is generally ≈0.05–0.5 mm [18, 19]. The high CTL in hybrid tapes thus explains the high NZPV observed.

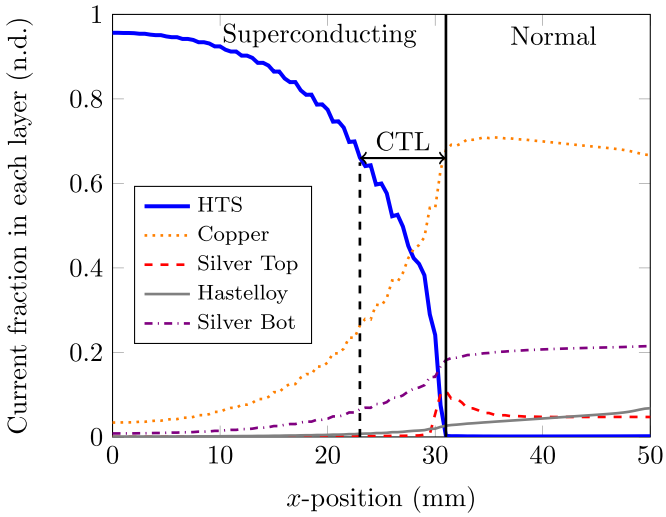

Figure 12. Fraction of the current flowing in the x-direction in each layer of the tape, close to the SC/NZ boundary. The vertical solid line located at $x = 31$ mm indicates the position where the current inside the HTS layer becomes zero (corresponding to the SC/NZ boundary), whereas the vertical dashed line located at $x = 23$ mm indicates the position where 63% (i.e. 1 - e^{-1}) of the current flows in the HTS layer.

Finally, numerical simulations were performed for the hybrid architecture, but with a much thicker copper layer on the substrate side, i.e. 40 μm instead of 3 μm in this paper. Stabilizers of 40 μm are commonly used in highly stabilized commercial tapes. A NZPV value of ≈100 cm s^{-1} was found at 155 A, which is one order of magnitude faster than what is measured on a conventional SCS4050 SuperPower sample (40 μm thick copper shunt, NZPV ≈ 7.7 cm s^{-1}), as reported in [9, 10].

6. Conclusion

The first important conclusion that we can draw from this paper is that the geometry of the metallic stabilizer has a major impact on the NZPV. Our results indicate that when copper is added on a commercial tape, it always reduces the NZPV in comparison to a bare tape. However, adding copper on the substrate side instead of the HTS side attenuates the reduction of the NZPV. This can be explained by the CFD effect induced by the buffer layers. Indeed, in this case, the current has to follow a more resistive path to reach the stabilizer when it is located under the substrate than when it is placed directly on top of the HTS layer. Therefore, if one needs to add copper to stabilize a tape, it is better to place it on the substrate in order to minimize the reduction of the NZPV.

The second important conclusion is that combining a bCFD architecture with a CFD on top of the tape greatly enhances the NZPV. We have shown in this paper that it is possible to increase the thickness of the stabilizer of a tape, while increasing at the same time its NZPV.

Therefore, the hybrid-CFD architecture is expected to be much more robust in case of a quench in both magnet and

power applications involving coils. This could also be a valuable solution to protect insulated coils from quenches, or at least to ease the design of the quench protection system.

Considering that the critical current of 2G HTS CCs is continuously increasing due to progress in fabrication processes, it is critical to find means to ensure the integrity of HTS tape for all types of events, and the results presented in this paper provide a promising solution to tackle this issue.

Acknowledgments

The authors would like to acknowledge NSERC and FRQNT for their financial support.

ORCID iDs

Christian Lacroix https://orcid.org/0000-0002-1648-1879
Jean-Hughes Fournier-Lupien https://orcid.org/0000-0002-0792-2548
Frédéric Sirois https://orcid.org/0000-0003-0372-9449

References

[1] Filipenko M *et al* 2020 *Supercond. Sci. Technol.* **33** 054002
[2] Bergen A *et al* 2019 *Supercond. Sci. Technol.* **32** 125006
[3] Godeke A *et al* 2020 *Supercond. Sci. Technol.* **33** 064001
[4] Bruzzone P, Fietz W H, Minervini J V, Novikov M, Yanagi N, Zhai Y and Zheng J 2018 *Nucl. Fusion* **58** 103001
[5] Hahn S *et al* 2019 *Nature* **570** 496–9
[6] Trillaud F, Palanki H, Trociewitz U, Thompson S, Weijers H and Schwartz J 2003 *Cryogenics* **43** 271–9
[7] Wang X, Trociewitz U P and Schwartz J 2007 *J. Appl. Phys.* **101** 053904
[8] Park H, Kim A, Park M, Yu I, Eom B, Bae J, Kim S, Sim K and Sohn M 2010 *IEEE Trans. Appl. Supercond.* **20** 2122–5
[9] van Nugteren J, Dhallé M, Wessel S, Krooshoop E, Nijhuis A and ten Kate H 2015 *Proc. 25th Int. Cryogenic Engineering Conf. and Int. Cryogenic Materials Conf. 2014 Phys. Proc.* **67** 945–51
[10] Bonura M and Senatore C 2016 *Appl. Phys. Lett.* **108** 242602
[11] Lacroix C and Sirois F 2014 *Supercond. Sci. Technol.* **27** 035003
[12] Lacroix C, Sirois F and Fournier-Lupien J-H 2017 *Supercond. Sci. Technol.* **30** 064004
[13] Fournier-Lupien J-H, Lacroix C, Hellmann S, Huh J, Pfeiffer K and Sirois F 2018 *Supercond. Sci. Technol.* **31** 125019
[14] SuperPower Inc. (2021) (www.superpower-inc.com/)
[15] Lacroix C, Lapierre Y, Coulombe J and Sirois F 2014 *Supercond. Sci. Technol.* **27** 055013
[16] Russek S E, Sanders S C, Roshko A and Ekin J W 1994 *Appl. Phys. Lett.* **64** 3649
[17] Levin G, Novak K and Barnes P 2010 *Supercond. Sci. Technol.* **23** 014021
[18] Polak M, Barnes P N and Levin G A 2006 *Supercond. Sci. Technol.* **19** 817
[19] Fournier-Lupien J-H, Lacroix C and Sirois F 2020 *Supercond. Sci. Technol.* submitted